

# Effects of Annealing Conditions on ZnO Buffer Layer for Inverted Polymer Solar Cells

Chuan Liu, Lihua Zheng, Zhiyang Gao, Yuhui Gan, Jian Zhang\*, Chuannan Li\*

State Key Laboratory on Integrated Optoelectronics, College of Electronic Science and Engineering,  
Jilin University, Qianjin Street, Changchun, China  
Email: \*zhangjian@jlu.edu.cn, \*licn@jlu.edu.cn

Received 2013

## ABSTRACT

A solution-processed zinc oxide (ZnO) thin film as the buffer layer with optimized processes especially the annealing conditions for inverted polymer solar cells (PSCs) has been demonstrated. Firstly the thickness of ZnO buffer layer was optimized, and different annealing conditions including temperature and time have also been taken into consideration. And the best Power Conversion Efficiency (PCE) 3.434% was observed when the ZnO buffer layer was spin-coated at 1500 rpm and annealed at 275°C for 5 min, and AFM results showed that morphology of this ZnO film has the best uniformity which was beneficial to form high quality polymer composite active layer.

**Keywords:** Polymer Solar Cells (PSCs); Zinc Oxide; Buffer Layer; Annealing; Morphology

## 1. Introduction

Polymer solar cells (PSCs) offer a potentially low-cost, lightweight, flexible and scalable source of renewable energy. However, before PSCs can become a marketable energy technology, further improvements on efficiency and stability are required. And the Power conversion efficiencies (PCEs) of PSCs have been improved through such as designs of the device structure, careful controls of morphology and the applications of low band gap materials [1-3]. And there exists significant interests in polymer bulk heterojunction solar cells by solution process due to their low temperature and high efficiency. In the regular bulk heterojunction PSCs structure, transparent indium tin oxide (ITO) usually is used as the anode and low work function metal as the cathode. Thus it brings the problem of low stability and efficiency. Therefore highly efficient polymer solar cells using an inverted structure, in which the positions of anode and cathode are reversed, have been demonstrated [4]. The low work function metal e.g. calcium used as the cathode in the regular structure, is replaced by a relatively nonreactive electron collection layer and transparent ITO film, and the stable metal such as Ag or Al can be used as the top anode of inverted PSCs, this significantly improves the air stability of the polymer solar cells. Furthermore, vertical phase separation in polymer blends has proven to be advantageous in the inverted structure [5].

One of the important keys to achieving high perform-

ance inverted PSCs is the selection of the electron collection layer between the transparent cathode and the active polymer composite layer. The purpose of the electron collection layer is to provide hole blocking capability and a low resistive pathway for efficiently electron extraction. Inorganic compounds CsCO<sub>3</sub> [6-7], TiO<sub>2</sub> [8,9] and ZnO [10] have been demonstrated as the effective electron collection materials. Particularly, solution-processed ZnO is an attractive candidate because it easily forms a nanostructure film with more efficient charge extraction and transporting capability, at the same time the solution-processed ZnO film reveals a strong hole blocking capability too [11]. During the fabrication processes of ZnO buffer layer, the rotating speed and annealing conditions greatly affect its electron collection and hole blocking characteristics, the formation of polymer composite active layer on ZnO film, and the performance of PSCs thereby [12,13].

Here we demonstrate the fabrication of inverted bulk heterojunction PSCs utilizing a ZnO interlayer as buffer layer between the ITO and active layer. The ZnO film is fabricated by solution processing, the morphology, IV characteristics with different annealing condition is thoroughly analyzed, and different annealing conditions on the ZnO buffer layer are optimized. And we also explore the best rotation speed of ZnO precursor solution for ZnO film.

## 2. Experiments

PSCs in these experiments were fabricated on patterned

\*Corresponding author.

ITO substrates which were ultrasonicated in acetone and isopropyl alcohol, followed by a 10 min UV-O<sub>3</sub> treatment before spin-coating. The ZnO precursor solution, consisting of 0.5 M zinc acetate dihydrate and 0.5 M monoethanolamine in 2-methoxyethanol, was first spin coated onto ITO substrates at different rpm for 40 seconds. Subsequently ZnO films are annealed at different conditions. Then the ZnO film was ultrasonicated in acetone and isopropyl alcohol for 5 min and dried at 200 °C for 5 min in order to remove the organic residuals of the ZnO film. The active layer for PSCs was spin coated from a 20 g/l solution of P3HT:PCBM 1:1 by weight in dichlorobenzene at 600 rpm for 1 min. The P3HT:PCBM active layer on ITO/ZnO combined film was annealed using a hot plate at 110°C for 10 min inner a nitrogen atmosphere, its thickness is about 230 nm. Finally a modified layer MoO<sub>3</sub> (4 nm) and top anode metal aluminum (80 nm) was vacuum-deposited onto the P3HT:PCBM active layer. The configuration of PSCs device structure is shown in **Figure 1**.

Devices were measured under simulated illumination at AM 1.5 G, 100 mW/cm<sup>2</sup> with a Keithley 2400 source meter controlled by a computer. The solar simulator was calibrated using a reference Si solar cell and all electrical measurements were carried out in air at room temperature. The surface morphologies of the photoactive layers were measured by atomic force microscopy (AFM). The

AFM images were obtained using a Veeco Dimension Icon system with tapping-mode.

### 3. Results and Discussions

Firstly, solar cells were fabricated with different rotation speed of ZnO, and then annealed under the two temperatures 200°C and 275°C, their current density-voltage (J-V) characteristics are shown in **Figures 2(a)** and **(b)**. And the performances of the solar cells are summarized in **Table 1**. For both two kinds of annealing conditions, the device shows a remarkable improvement with 1500 rpm of ZnO film compared to the devices with other spin-coating speeds. For device annealed at 200°C for 1 hour,

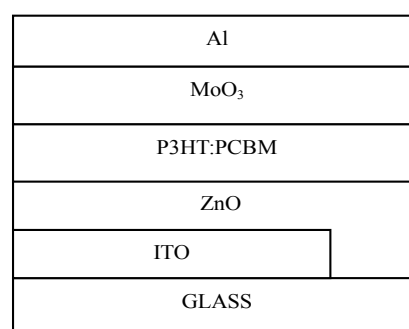


**Figure 1.** Configuration of the inverted PSCs device structure.

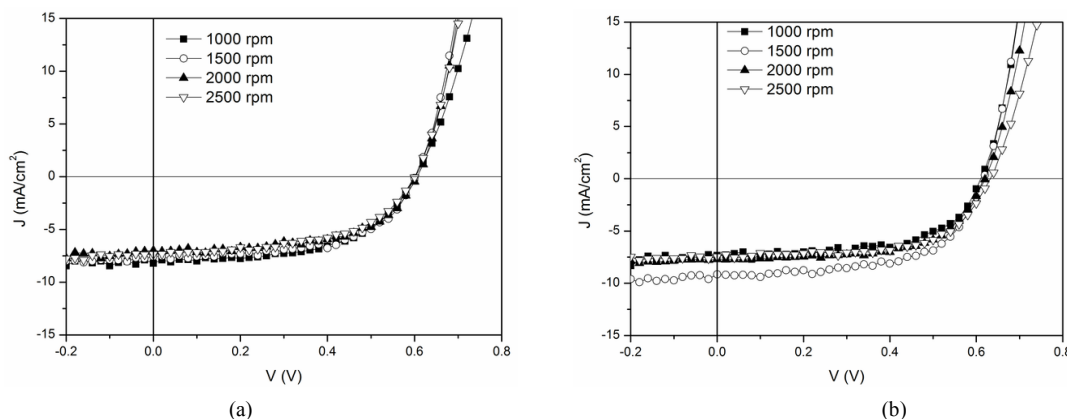


**Figure 2.** J-V characteristics of devices with ZnO film by different spin-coating speeds and annealing at (a) 200°C for 1 h and (b) 275°C for 5 min.

**Table 1.** Summarized performance characteristics of polymer solar cells with different spin-coating speeds and annealing temperatures.

Rotating speed of ZnO (rpm)	Annealing Condition	V <sub>oc</sub> (V)	J <sub>sc</sub> (mA/cm <sup>2</sup> )	FF (%)	PCE (%)
1000	200°C, 1h	0.6	8.203	54.69	2.692
1500	200°C, 1h	0.60	7.567	59.84	2.717
2000	200°C, 1h	0.61	6.999	59.04	2.501
2500	200°C, 1h	0.60	7.343	54.03	2.380
1000	275°C, 5min	0.61	7.342	61.42	2.751
<b>1500</b>	<b>275°C, 5min</b>	<b>0.62</b>	<b>9.152</b>	<b>60.53</b>	<b>3.434</b>
2000	275°C, 5min	0.62	7.771	62.03	2.964
2500	275°C, 5min	0.63	7.450	62.94	2.954

the short circuit current density ( $J_{SC}$ ) is  $7.567 \text{ mA/cm}^2$ , the open circuit voltage ( $V_{OC}$ ) is equal to  $0.60 \text{ V}$ , and the filling factor (FF) is  $59.84\%$ , resulting in a PCE of  $2.717\%$ . At the same time when the annealing condition is  $275^\circ\text{C}$  for  $5 \text{ min}$ , the  $J_{SC}$ ,  $V_{OC}$ , FF and PCE is  $9.152 \text{ mA/cm}^2$ ,  $0.62 \text{ V}$ ,  $60.53\%$  and  $3.434\%$  respectively.

**Figure 3(a)** is the AFM height images of the ZnO film spin coated at  $1500 \text{ rpm}$  and annealed at  $200^\circ\text{C}$  for  $1 \text{ h}$ . And **Figure 3(c)** shows the height image of ZnO film annealed at  $275^\circ\text{C}$  for  $5 \text{ min}$ . The r.m.s. roughness of **Figure 3(a)** is  $3.39 \text{ nm}$ , and **Figure 3(c)** shows an r.m.s. roughness of about  $1.36 \text{ nm}$ , which is much smoother than the former. **Figure 3(b)** and **(d)** show the AFM phase image of the ZnO buffer layer annealed at  $200^\circ\text{C}$  for  $1 \text{ h}$  and  $275^\circ\text{C}$  for  $5 \text{ min}$  respectively. It also shows that annealing at  $275^\circ\text{C}$  for  $5 \text{ min}$  can form a homogeneous ZnO film evenly distributing on the ITO. All these provide a better condition to deposit a high quality polymer composite active film, and enhance their combination of the ZnO buffer layer and the polymer composite active layer. As a result, it improves the efficiency of the device by means of increasing the photogenerated electrons transmitted to the electrode through ZnO buffer layer.

Then the ZnO film is annealed at  $200^\circ\text{C}$  and  $275^\circ\text{C}$  for different times in order to optimize the annealing condition.

The performances of the solar cells are summarized in

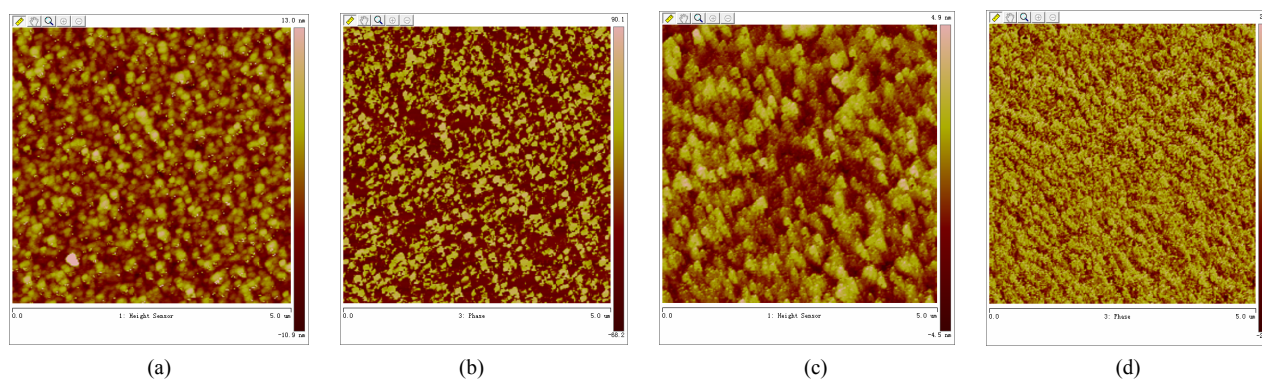


**Figure 3.** (a) AFM height image and (b) phase image of ZnO film annealed at  $200^\circ\text{C}$  for  $1 \text{ h}$ , (c) AFM height image and (d) phase image of ZnO film annealed at  $275^\circ\text{C}$  for  $5 \text{ min}$ .

**Table 2.** Summarized performance characteristics of polymer solar cells with different annealing time.

Annealing temperature ( $^\circ\text{C}$ )	Time (min)	$V_{OC}$ (V)	$J_{SC}$ ( $\text{mA/cm}^2$ )	FF (%)	PCE (%)	$R_S$ ( $\Omega \cdot \text{cm}^2$ )	$R_{SH}$ ( $\Omega \cdot \text{cm}^2$ )
200	20 (A)	0.59	8.490	57.95	2.693	3.989	243.9
200	40 (B)	0.60	8.536	57.70	2.955	6.169	1368.3
200	60 (C)	0.59	7.567	59.84	2.717	2.315	264.3
200	80 (D)	0.60	7.252	36.99	1.610	36.53	207.5
<b>275</b>	<b>5 (E)</b>	<b>0.62</b>	<b>9.152</b>	<b>60.53</b>	<b>3.434</b>	<b>1.996</b>	<b>1976</b>
275	10 (F)	0.62	7.857	58.93	2.871	6.163	519.2
275	15 (G)	0.60	7.653	58.55	2.733	5.975	460.9
275	20 (H)	0.61	7.318	58.29	2.602	4.906	304.8

**Table 2.** **Figures 4(a)** and **(b)** show the dark characteristics and J-V characteristics of the devices with ZnO buffer layer annealed at  $200^\circ\text{C}$  for different times ( $20 \text{ min}$  marked as device A,  $40 \text{ min}$  as device B,  $60 \text{ min}$  as device C,  $80 \text{ min}$  as device D). From **Figure 4(a)**, the current density under forward biases of device B and C is much higher than device A and D, this means device B and C have a better injection capability. But the current density at reversed biases from device C is lower than the device B, which implies a lower leakage current, and when applied voltage located from  $0 \text{ V}$  to  $0.4 \text{ V}$ , device C has a largest current density. Therefore device C has the largest  $R_{SH}$  ( $1368.3 \Omega \cdot \text{cm}^2$ ), shown in Table II. That indicates device C has the largest  $J_{SC}$  and good FF which can be seen in **Figure 4(b)**. So when the annealing temperature is  $200^\circ\text{C}$  and annealing time is  $40 \text{ min}$ , devices have the highest efficiency which is  $2.955\%$ .

**Figure 4(c)** and **(d)** show the J-V characteristics and dark characteristics of the devices with ZnO buffer layer annealed at  $275^\circ\text{C}$  for different times ( $5 \text{ min}$  marked as device E,  $10 \text{ min}$  as device F,  $15 \text{ min}$  as device G, and  $20 \text{ min}$  as device H). From Fig. 4c, the current density at forward biases decreases with the increase of annealing time, which shows the device E has the best injection characteristic. So the device E shows the largest  $R_{SH}$  ( $1976 \Omega \cdot \text{cm}^2$ ) and the lowest  $R_S$  ( $1.996 \Omega \cdot \text{cm}^2$ ). Therefore when the annealing time is  $5 \text{ min}$ , the device E has the highest efficiency which is  $3.434\%$ .

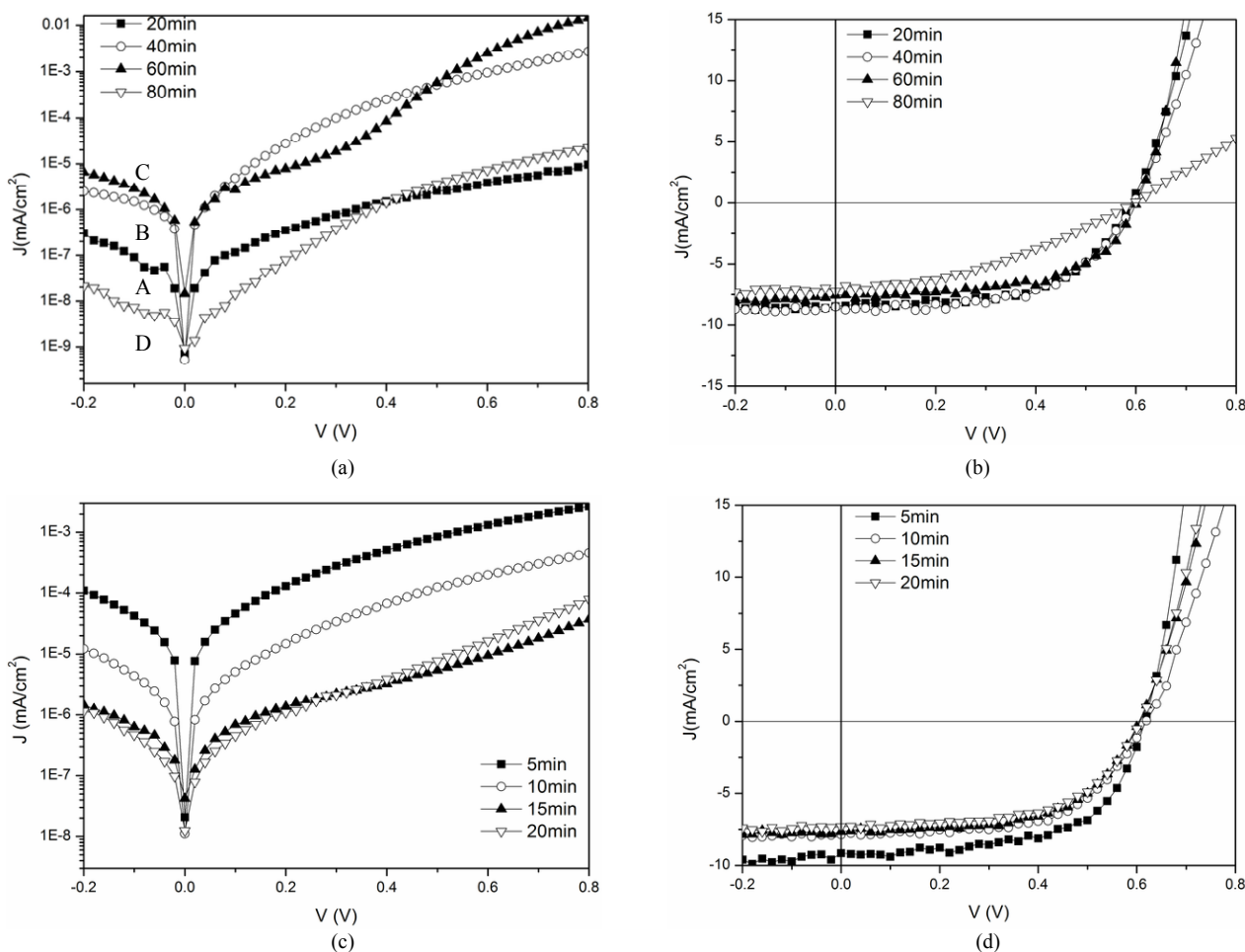


**Figure 4.** Dark current characteristics and J-V characteristics of the Devices with ZnO annealing at 200°C for different time (a, b), and the devices with ZnO annealing at 275°C for different time (c,d).

## 5. Conclusions

Inverted PSCs with a ZnO buffer layer between the ITO cathode and the polymer composite P3HT:PCBM was fabricated. Firstly the ZnO buffer layer was spin coated using ZnO precursor solution at different rotation speeds in order to form ZnO film with optimized thickness, and the PCE of the PSCs reached 3.434% with the rotation speed 1500 rpm. The various annealing temperature and times were studied, and the devices annealed at a higher temperature 275°C showed a higher PCE than that annealed at 200°C. Moreover, when the annealing temperature is 275°C the PCE of devices decreased with the increase of annealing time. Consequently, the device with the ZnO film spin coated at 1500 rpm and annealed 275°C for 5 min showed the highest PCE 3.434%, owing to the formation of the optimal ZnO buffer layer film.

## 6. Acknowledgements

This work was supported by the National Natural Science Foundation of China (NSFC) under Grant 61177025

and National Training Programs of Innovation and Entrepreneurship for Undergraduates of China under Grant 2012A51130.

## REFERENCES

- [1] G. Li, R. Zhu and Y. Yang, "Polymer Solar Cells," *Nature Photonics*, Vol. 6, 2012, pp. 153-161.
- [2] G. Li, V. Shrotriya, J. Huang and Y. Yao, "High-Efficiency Solution Processable Polymer Photovoltaic Cells by Self-Organization of Polymer Blends," *Nature Materials*, Vol. 4, 2005, pp. 864-868. [doi:10.1038/nmat1500](https://doi.org/10.1038/nmat1500)
- [3] J. Peet, J. Y. Kim and N. E. Coates, "Efficiency Enhancement in Low-Bandgap Polymer Solar Cells by Processing with Alkane Dithiols," *Nature Materials*, Vol. 6, 2007, pp. 497-500. [doi:10.1038/nmat1928](https://doi.org/10.1038/nmat1928)
- [4] L.M. Chen, Z. Hong, G. Li and Y. Yang, "Recent Progress in Polymer Solar Cells: Manipulation of Polymer: Fullerene Morphology and the Formation of Efficient Inverted Polymer Solar Cells," *Advanced Materials*, Vol. 21, 2009, pp. 1434-1449.

- [doi:10.1002/adma.200802854](https://doi.org/10.1002/adma.200802854)
- [5] Z. Xu, L. M. Chen and Y. Yang, "Vertical Phase Separation in Poly(3-hexylthiophene): Fullerene Derivative Blends and its Advantage for Inverted Structure Solar Cells," *Advanced Functional Materials*, Vol. 19, No. 8, 2009, pp. 1227-1234. [doi:10.1002/adfm.200801286](https://doi.org/10.1002/adfm.200801286)
- [6] H. H. Liao, L. M. Chen, Z. Xu, G. Li and Y. Yang, "Highly Efficient Inverted Polymer Solar Cell by Low Temperature Annealing of Cs<sub>2</sub>CO<sub>3</sub> Interlayer," *Applied Physics Letters*, Vol. 92, 173303, 2008.
- [7] G. Li, C.-W. Chu and V. Shrotriya, "Efficient Inverted Polymer Solar Cells," *Applied Physics Letters*, Vol. 88, 253503, 2006.
- [8] G.K. Mor, K. Shankar, M. Paulose, O.K. Varghese and C.A. Grimes, "High Efficiency Double Heterojunction Polymer Photovoltaic Cells Using Highly Ordered TiO<sub>2</sub> Nanotube Arrays," *Applied Physics Letters*, Vol. 91, 152111, 2007.
- [9] C. Waldauf, M. Morana, P. Denk and P. Schilinsky, "Highly Efficient Inverted Organic Photovoltaics Using Solution Based Titanium Oxide as Electron Selective Contact," *Applied Physics Letters*, Vol. 89, 233517, 2006.
- [10] M. S. White, D. C. Olson, S. E. Shaheen, N. Kopidakis and D. S. Ginley, "Inverted Bulk-Heterojunction Organic Photovoltaic Device Using A Solution-derived ZnO Underlayer," *Applied Physics Letters*, Vol. 89, 143517, 2006.
- [11] L. Vayssieres, "Growth of Arrayed Nanorods and Nanowires of ZnO from Aqueous Solutions," *Advanced Materials*, Vol. 15, No. 5, 2003, pp. 464-466. [doi:10.1002/adma.200390108](https://doi.org/10.1002/adma.200390108)
- [12] N. Sekine, C.-H. Chou, W. L. Kwan and Y. Yang, "ZnO Nano-Ridge Structure and Its Application in Inverted Polymer Solar Cell," *Organic Electronics*, Vol. 10, 2009, pp. 1473-1477. [doi:10.1016/j.orgel.2009.08.011](https://doi.org/10.1016/j.orgel.2009.08.011)
- [13] T. B. Yang, W. Z. Cai, D. H. Qin and Y. Cao, "Solution-Processed Zinc Oxide Thin Film as a Buffer Layer for Polymer Solar Cells with an Inverted Device Structure," *Journal of Physical Chemistry C*, Vol. 114, 2010, pp. 6849-6853. [doi:10.1021/jp1003984](https://doi.org/10.1021/jp1003984)